Available online at www.sciencedirect.com
ScienceDirect
Journal of the European Ceramic Society 29 (2009) 2937–2943
www.elsevier.com/locate/jeurceramsoc

Fabrication and characterization of 45S5 bioglass reinforced macroporous calcium silicate bioceramics

Kaili Lin, Jiang Chang *, Ziwei Liu, Yi Zeng, Ruxiang Shen

Biomaterials and Tissue Engineering Research Center, Shanghai Institute of Ceramics, Chinese Academy of Sciences, 1295 Dingxi Road, Shanghai 200050, PR China

Received 4 December 2008; received in revised form 19 April 2009; accepted 22 April 2009
Available online 21 May 2009

Abstract

Bioactive and degradable macroporous bioceramics play an important role in clinical applications. In the present study, 45S5 bioglass reinforced macroporous calcium silicate ceramics (45BG-reinforced MCSCs) were fabricated. The effect of bioglass additives on compressive strength and open porosity of the samples was investigated, and the bioactivity and degradability of the obtained reinforced samples were also evaluated. The 45S5 bioglass additive was found to be effective to increase the strength of the MCSCs by the liquid-phase sintering mechanism. The optimum amount of bioglass additives was 5 wt.% and the compressive strength of the reinforced samples was approximately 2 times higher as compared to the pure macroporous calcium silicate ceramics (MCSCs). The compressive strength of the reinforced samples with about 50% porosity reached 112.47 MPa, which was similar to those of the cortical bones. After soaking in simulated body fluid (SBF), hydroxycarbonate apatite (HCA) layer was formed on the surface of the 45BG-reinforced MCSCs. Furthermore, the degradation rate of the reinforced samples was just about one-third of those pure MCSCs. Our results indicated that degradable 45BG-reinforced MCSCs possess excellent mechanical strength and bioactivity, and may be used as bioactive and degradable biomaterials for hard tissue prosthetics or bone tissue engineering applications.

Keywords: Macroporous calcium silicate; Mechanical properties; Glass; Biomedical applications; Reinforcement

1. Introduction

Three-dimensional (3D) macroporous bioceramics have received considerable attention as their important role in hard tissue repair and tissue engineering. Hench et al. pointed out that the main characteristics of the third-generation biomaterials are bioactivity and biodegradability.[1] The bioactivity can enhance the in-growth of bone tissue to achieve full integration with the living bone tissues.[1–3] After implantation, the implants were biodegraded in time with the tissue in-growths. Moreover, the proper mechanical strength is required in order to maintain the shape against the stress during the surgical procedure and recovery. However, the inherently low mechanical strength of ceramics, such as macroporous apatite ceramics has severely hindered their clinical applications.[4]

In recent years, calcium silicate ($CaSiO_3$, CS) ceramics have been investigated as a new type bioceramics for hard tissue regeneration.[5–7] A few studies have shown that CS materials are bioactive and can quickly induce formation of a bonelike apatite layer on their surface after soaking in simulated body fluid,[8–11] in the cell culture situation,[12] and after implantation *in vivo*.[6,7] Our previous studies revealed that the bone-regeneration ability and biodegradability of CS bioceramics were faster than that of β-tricalcium phosphate bioceramics,[7] and thereby might be applied in hard tissue repair or as 3D scaffolds for tissue engineering.

The macroporous calcium silicate ceramics (MCSCs) have been prepared by porogen burning-out method.[13] The results showed that the compressive strength of the MCSCs with 250–500 μm macropore sizes and 41.28–73.60% porosities could be controlled between 4.92 and 58.23 MPa. The compressive strength was much lower than that of cortical bones.[14] Therefore, it is an important task to fabricate high mechanical strength macroporous bioceramic scaffolds with high porosity, which will broaden its application field as bone implant materials.

It has been well recognized that the liquid-phase sintering route using glasses as sintering additives is an effective way to

* Corresponding author. Tel.: +86 21 52412804; fax: +86 21 52413903.
E-mail address: jchang@mail.sic.ac.cn (J. Chang).

0955-2219/$ – see front matter © 2009 Elsevier Ltd. All rights reserved.
doi:10.1016/j.jeurceramsoc.2009.04.025

improve the mechanical properties in engineering ceramics and bioceramics.[15,16] The glassy phase, which has a lower melting point compared with the major phase, is liquid during the sintering process of the ceramic matrix. Such additives can promote liquid-phase formation at lower sintering temperatures and may considerably increase the rate of sintering. During the sintering process, a viscous liquid may promote an additional diffusion mechanism of dissolution/precipitation, particle rearrangement and capillary forces and finally may improve the densification. The improvement of the densification ultimately results in the increase of the mechanical properties.[15,17] However, up to now, most works were focused on the glassy phase sintering behaviors and their influences on the properties of the dense ceramics,[15,16,18] few works have been carried out on the reinforcement behavior of glass on the porous ceramics. In addition, it is also assumed that the presence of bioactive glassy phase can provide faster response in terms of bone healing and bonding processes.[19] 45S5 bioglass possesses excellent bioactivity, biocompatibility and degradability, and showed a strong chemical bonding with the neighbouring tissues *in vivo*.[14,21] Therefore, in this study, the 45S5 bioglass was used as glassy phase to reinforce the MCSCs. The effects of the 45S5 bioglass on the mechanical strength and open porosity of the fabricated samples were investigated, and the in vitro bioactivity and degradability of the obtained samples were evaluated by soaking in simulated body fluid (SBF).

2. Materials and methods

2.1. Preparation of $CaSiO_3$ powders and 45S5 bioglass powders

The $CaSiO_3$ powders were prepared as previously described.[13] Briefly, 1000 mL of 0.4 mol $Ca(NO_3)_2$ solution with a pH 11.4 was vigorously stirred at room temperature, and 1000 mL of 0.4 mol Na_2SiO_3 was added dropwise to this solution over a period of 40–60 min resulting in a white precipitate. The white precipitate was stirred for 24 h, washed 4 times with distilled water to remove the Na^+ and NO_3^- ions, and then washed twice with 100% ethanol to improve the dispersion characteristics. After washing, the remaining liquid was removed by vacuum filtration, and the precipitate was dried at 80 °C for 24 h. β-$CaSiO_3$ was obtained by calcining the powders at 800 °C. The obtained $CaSiO_3$ powders were sieved to obtain particles of size 38–45 μm. The 45S5 bioglass was prepared using the following analytical grade oxides: 45 wt.% SiO_2, 6 wt.% P_2O_5, 24.5 wt.% Na_2O and 24.5 wt.% CaO. The mixtures were placed in a platinum crucible and heated to 1330 °C for 4 h. Subsequently they were poured into water to obtain granules.[14] They were milled and sieved to obtain particles of size 38–45 μm.

2.2. Fabrication and characterization of the 45BG-reinforced MCSCs

The composites of $CaSiO_3$ and 45S5 bioglass powders with 45S5 bioglass varying in content from 0 to 10 wt.% were mechanically ball milled in 100% ethanol for 24 h using high-purity alumina media. After drying, they were sieved through a 120-μm screen. 6 wt.% polyvinyl alcohol solution was added into the mixtures as a binder and the mixtures were mechanically mixed with 300–600 μm polyethylene glycol (PEG) particulates. The mixture was dry pressed under a uniaxial pressure of 14 MPa in a stainless steel die. In order to obtain substrates with different porosities, different amounts of PEG were used. The additives, PEG, functioned as a sacrificial agent during sintering. During firing, the PEG burned off, leaving behind a network of pores throughout the disks. The green disks with a diameter of 10 mm and a thickness of 4 mm were heat treated at 400 °C for 2 h at a firing rate of 2 °C/min to drive off the porogens, sintered at 1100 °C for 3 h at a firing rate of 2 °C/min and then cooled to room temperature at a rate of 2 °C/min in the furnace.

To investigate the pore structures, the cross-section of the sintered samples was observed by scanning electron microscopy (SEM; Shimadzu EPMA-8705QHII, Japan), and the macropore size was estimated from the SEM images. The open porosity of the sintered samples was determined by the Archimedian method.[21] The phase of the sintered samples was determined by X-ray diffraction (XRD, Geigerflex, Rigaku Co., Japan). The compressive strength of the sintered samples was measured using a mechanical testing machine (Shimadzu AG-5kN, Japan) at a crosshead speed of 0.5 mm/min. In this study, five pieces from each group were tested to obtain the average compressive strength and open porosity.

2.3. Evaluation of bioactivity and degradability in simulated body fluid (SBF)

The bioactivity of the fabricated 45BG-reinforced MCSCs (with 5 wt.% reinforcement and 40 wt.% porogens) was evaluated by examining the bonelike hydroxyapatite (HAp) formation on the samples in SBF,[22] which was prepared as previously described by Kokubo and had similar ion concentrations to those in human blood plasma (Table 1). Briefly, analytical reagent grade NaCl, $NaHCO_3$, KCl, K_2HPO_4, $MgCl_2$, $CaCl_2$ and Na_2SO_4 were dissolved in distilled water and the solution was buffered to pH 7.4 at 37 °C with tris(hydroxymethyl) aminomethane and hydrochloric acid.

The samples were soaked in the SBF for different periods at 37 °C with the ratio of mass to solution volume of 0.15 g/30.0 mL. The SBF solutions were refreshed every 24 h. After various soaking periods, the samples were removed from the SBF solution, gently rinsed with distilled water, and then dried at room temperature before further characterization. The formation of bonelike HAp on the surface of the samples was characterized by XRD and Fourier transform infrared

Table 1
Ion concentration of SBF in comparison with human blood plasma.

Types	Ion concentrations (mM)						
	Na^+	K^+	Mg^{2+}	Ca^{2+}	Cl^-	HCO_3^-	HPO_4^{2-}
SBF	142.0	5.0	1.5	2.5	148.8	4.2	1.0
Blood plasma	142.0	5.0	1.5	2.5	103.0	27.0	1.0

spectroscopy (FTIR; Nicolet Co., USA) using KBr technology, and the morphology of the samples was observed using field emission scanning electron microscope (FESEM; JSE-6700F, JEOL, Japan).

To evaluate the degradability of the fabricated bioceramics, the samples were soaked in the SBF without refreshing the soaking medium. After various soaking periods, the samples were removed and the concentrations of Si in the SBF solutions after soaking were determined by inductively coupled plasma atomic emission spectroscopy (ICP-AES; Varian Co., USA). Considering the fact that Si is absent from SBF before soaking, the degradation rate (S) of the samples in different time periods was calculated by the following equation:

$$S\,(\%) = \frac{c_{\mathrm{Si}} \times v}{m_{\mathrm{Si}}} \times 100$$

where c_{Si}, v, and m_{Si} represent the Si concentration in SBF (mg/mL), volume of SBF (mL) and Si content (mg) of the samples soaked in SBF, respectively.

3. Results and discussion

3.1. Characterizations of the 45BG-reinforced MCSCs

The effect of the 45S5 bioglass additive amount on the linear shrinkage, open porosity and compressive strength of the sintered MCSCs is shown in Table 2. With the increase of 45S5 bioglass additives, the ratio of linear shrinkage increased gradually. This phenomenon could be explained as follows: the 45S5 bioglass additives melted into liquid-phase during the sintering. The distance between the $CaSiO_3$ particles decreased owing to the capillary force and consequently resulted in the specimen shrinkage. More liquid-phase would cause more shrinkage of the prepared samples. With the variation of the additive amount, the open porosity of the ceramics also changed, as shown in Table 2. The existence of glass phase effectively increased the packing density of the $CaSiO_3$ particles in the solid wall due to the capillary force of the liquid-phase sintering mechanism. In contrast, the compressive strength of the fabricated 45BG-reinforced MCSCs increased slightly with an increase in the additive amount from 0 to 3 wt.%. It increased sharply with further increase in the additive amount to 5 wt.% and reached a maximal value of 112.47 MPa, which was 2.32 times higher than that of the pure MCSCs. The compressive strength slightly decreased with further increase in the additive amount up to 10 wt.%. There was no significant improvement in maximum strength for samples with 1–3 wt.% additives, since no enough liquid-phase was formed during the sintering. Therefore, it can be assumed that the optimum amount of the 45S5 bioglass additives is about 5 wt.%. When the additive amount increased from 0 to 5 wt.%, the open porosity of the samples decreased slightly from 53.69% to 50.10%, but the mechanical strength increased remarkably from 48.51 to 112.47 MPa. In order to investigate the role of 45S5 bioglass in the reinforcement of the MCSCs, the pure MCSCs with a similar pore size distribution and an open porosity of 50.13% were fabricated using 37.3 wt.% porogens. As shown in Table 2, less porogens were required for the fabrication of the pure MCSCs than for the 45BG-reinforced MCSCs with similar open porosity, this suggested that the additives of 45S5 bioglass could increase the densification of the solid wall of the sintered samples, and ultimately resulted in slightly less open porosity. When the open porosity of the pure MCSCs decreased from 53.69% to 50.13%, the compressive strength only increased from 48.51 to 51.95 MPa. The open porosities of both samples decreased by approximately 3.5%, but the increment in the mechanical strength of the reinforced samples with 5 wt.% 45S5 bioglass was approximately 18 times higher than that of the pure MCSCs. These phenomena suggested that the liquid-phase sintering improved the densification of the solid wall of the fabricated samples, which remarkably increased the mechanical strength of the MCSCs with 45S5 bioglass reinforcement.

Fig. 1 shows the SEM micrographs of the fractured surface of the prepared pure MCSCs and 5 wt.% 45BG-reinforced MCSCs fabricated using 50 wt.% of porogens. Both of the samples were highly porous with evenly distributed and interconnected pores. The shapes of pores were similar to those of the PEG particulates, and the macropore sizes were about 250–500 μm. It is obvious that the macropores created by porogens had an average shrinkage by ~15% in size after sintering and this might be attributed to the densification effect, particularly for the fine $CaSiO_3$ powders.[12] Fig. 1C and 1D shows the microstructures of the solid walls of the pure MCSCs and 5 wt.% 45BG-reinforced MCSCs, respectively. It is clear to see that the solid walls of the pure MCSCs consist poorly densified bodies with a large number of intergranular micro-pores in the size of 0.5–5 μm. On the contrary, the 45S5 bioglass could apparently increase the solid wall density (Fig. 1D). The increase of the solid wall density resulted in the slight decrease of the porosity of the fabricated samples, which was consistent with the porosity data shown

Table 2
Effect of the 45S5 bioglass additive amount on the linear shrinkage, open porosity and compressive strength of the prepared samples (the samples were fabricated by mixing $CaSiO_3$ powders with 40 wt.% PEG particulates, except that indicated by *, which was fabricated by mixing $CaSiO_3$ powders with 37.3 wt.% PEG).

Additive amount (wt.%)	Sintered at 1100 °C for 3 h		
	Linear shrinkage (%)	Open porosity (%)	Compressive strength (MPa)
0	8.63 ± 0.58	53.69 ± 1.54	48.51 ± 4.94
1	8.75 ± 0.37	53.33 ± 1.79	50.80 ± 3.62
3	8.86 ± 0.10	52.02 ± 2.27	68.94 ± 2.89
5	8.94 ± 0.62	50.10 ± 1.97	112.47 ± 6.53
10	8.99 ± 0.25	49.52 ± 1.08	109.26 ± 7.37
0*	8.66 ± 0.45*	50.13 ± 1.85*	51.95 ± 3.71*

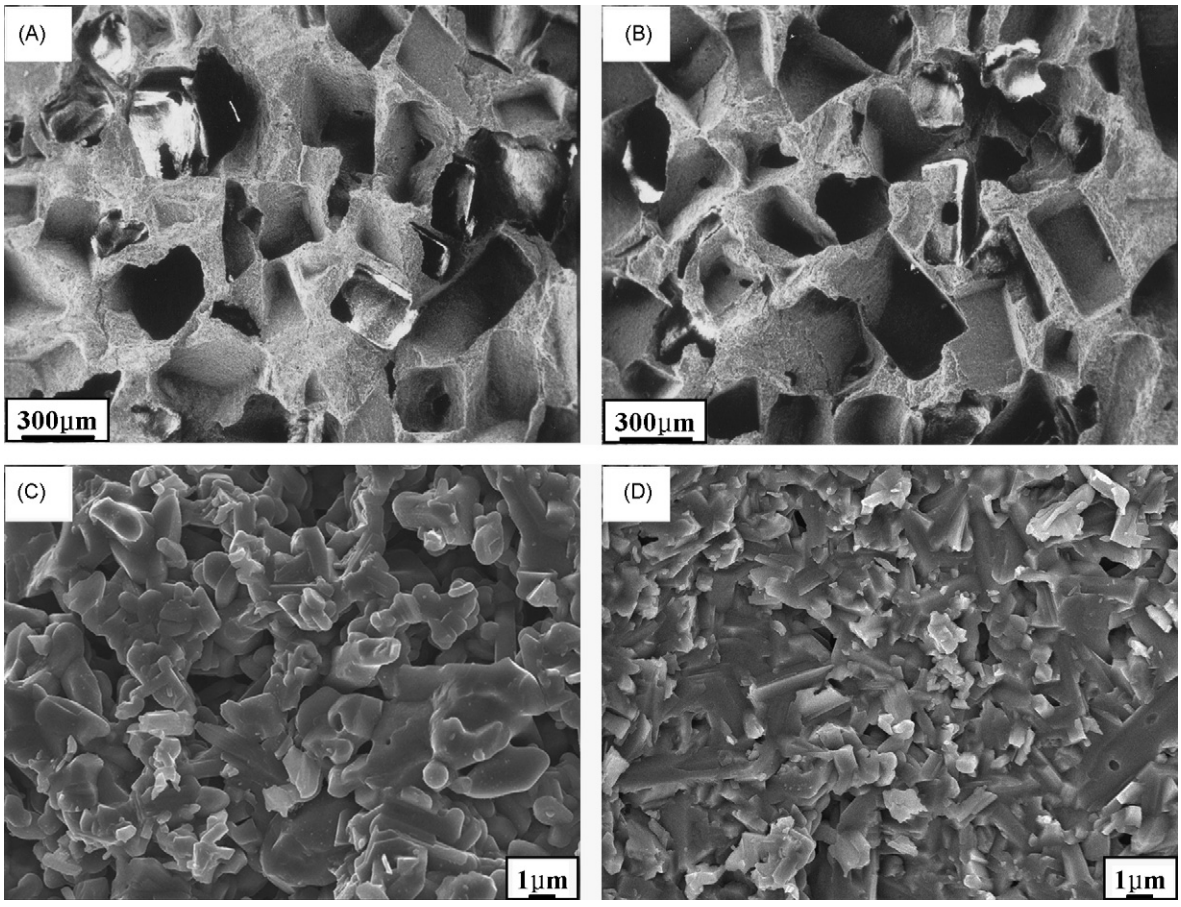

Fig. 1. SEM micrographs of the fractured surface of the pure MCSCs (A and C) and 5 wt.% 45S5 bioglass reinforced MCSCs (B and D).

in Table 2. Moreover, the numbers of micro-pores in 45BG-reinforced MCSCs are considerable fewer than those in pure MCSCs. The apparent increase in the solid wall density and the slight decrease in porosity remarkably increased the mechanical properties of the sintered matrixes.

Fig. 2 shows the XRD patterns of the 5 wt.% 45BG-reinforced MCSCs samples sintered at 1100 °C for 3 h. It can be seen that the fabricated 45BG-reinforced MCSCs were composed of α-$CaSiO_3$, which suggested that the presence of 5 wt.% of 45S5 bioglass did not alter the phases of the MCSCs.

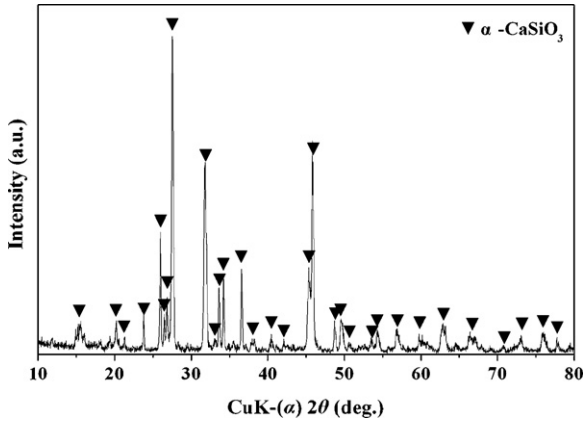

Fig. 2. XRD patterns of the samples with 5 wt.% 45S5 bioglass sintered at 1100 °C for 3 h.

Table 3 shows the effect of the 5 wt.% bioglass additives on the compressive strength and open porosity of the ceramics prepared by mixing different amount of porogens. The open porosities increased as the weight fraction of the PEG porogens increased. An increase of 10 wt.% of porogens could result in about 10% increase in the open porosity. The open porosities of the samples with 5 wt.% additives were slightly lower than that of the pure samples, which was due to the liquid-phase sintering mechanism and resulted in a higher solid wall density. It is clear to see that the 5 wt.% additives could effectively increase the mechanical strength of the MCSCs at different porosities. The compressive strength of the samples reinforced by 5 wt.% bioglass was approximately 2 times stronger than that of the pure MCSCs. Even at the high porosity of 71.12%, the compressive strength of the samples reinforced by 45S5 bioglass reached 8.74 MPa. The decrease of the mechanical strength has always been a serious concern in porous ceramics. In general, the porosity is one of the key factors affecting the mechanical strength of the porous ceramics. The strength of ceramics increases obviously with a decrease in porosity.[23] With 5 wt.% 45S5 bioglass additives, the samples with 50.10% porosity were almost 13 times stronger than the samples with 71.12% porosity. With 5 wt.% 45S5 bioglass additives, the compressive strength and the open porosity of the MCSCs could

Table 3
Effect of the 5 wt.% additives on the compressive strength and open porosity of the prepared samples (the samples were prepared by mixing $CaSiO_3$ powders with 40, 50 and 60 wt.% PEG particulates).

Samples	Sintered at 1100 °C for 3 h					
	40 wt.% PEG		50 wt.% PEG		60 wt.% PEG	
	Open porosity (%)	Compressive strength (MPa)	Open porosity (%)	Compressive strength (MPa)	Open porosity (%)	Compressive strength (MPa)
0 wt.% additives	53.60 ± 1.54	48.51 ± 4.94	64.20 ± 3.16	20.33 ± 2.07	73.60 ± 1.87	4.92 ± 0.83
5 wt.% additives	50.10 ± 1.97	112.47 ± 6.53	61.30 ± 1.69	37.84 ± 2.16	71.12 ± 2.38	8.74 ± 0.76

be controlled from 8.74 to 112.47 MPa and from 50.10% to 71.12%, respectively, by regulating the weight fraction of the porogens. Ioku et al. have investigated the compressive strength of macroporous HAp, β-TCP and HAp/β-TCP composite bioceramics with ~60% porosity and macropore size distribution between 150 and 400 μm.[24] Their study showed that the compressive strength of the porous HA, β-TCP and HA/β-TCP bioceramics was between 12.5 and 21.4 MPa. In our study, the fabricated 45BG-reinforced MCSCs with similar porosity and much larger pore size distributions showed a compressive strength of 37.84 MPa (Table 3), which was about 1.8–3.0 times higher than that of the HA, β-TCP and HA/β-TCP bioceramics. The results showed that the mechanical strength of 45BG-reinforced MCSCs was much higher than that of macroporous apatite bioceramics, pure MCSCs and other biocompatible macroporous glass and glass–ceramics reported in the literatures so far. The compressive strength of the reinforced samples with 50.10% porosity reached 112.47 MPa, which was similar to that of the cortical bones,[20] and therefore the reinforced samples might be used as load-bearing materials for hard tissue prosthetics applications.

3.2. Evaluation of the in vitro bioactivity and degradability

Fig. 3 showed the FESEM micrographs of 45BG-reinforced MCSCs soaked in SBF for 0 and 1 day. The surface of the samples soaked in SBF for 1 day was completely covered by ball-like particles (Fig. 3B). The high magnification image inserted in Fig. 3B shows that the ball-like particles consisted of a fine structure of nano-particles with sizes in about 80 nm.

Fig. 4 shows the XRD patterns of the samples after soaking in SBF for 7 days. It can be seen that, broad diffraction patterns ascribed to low crystalline apatite were observed at 2θ of 25.9° and 31.7°, and the peaks of α-$CaSiO_3$ disappeared completely.

Fig. 5 presents the FTIR spectra of the samples soaked in SBF for 0, 1, 3 and 7 days. As observed, the intensity of the silicate absorption bands at 474 cm^{-1} decreased when the soaking periods increased. Simultaneously, new absorption bands at 604 and 565 cm^{-1} can be recognized after soaking for 1 day, which were caused by the bending vibration mode of the PO_4^{3-} group and suggested the formation of hydroxyapatite.[25] A very broad OH^- absorption bands from 3700 to 2500 cm^{-1} and a weak water absorbed band around 1635 cm^{-1} appeared in these spectra. Bands between 1400 and 1550 cm^{-1} were considered for the absorption of carbonate group (υ_3). The peaks around 876 cm^{-1} was due to the joint contribution of CO_3^{2-} and HPO_4^{2-} ions,[26] and the broad bands from 900 to 1300 cm^{-1} were mainly attributed to the phosphate absorption.[26] In addition, the bands at around 565, 604 and 900–1300 cm^{-1} were the characteristic of HAp crystals.[27]

It is obvious from the results described above that the 45BG-reinforced MCSCs could develop a bonelike hydroxycarbonate apatite (HCA) layer on the surface when soaked in SBF. The bonelike HCA layer, which precipitates on the surface of a bioactive material *in vivo*, is considered to play an essential role in the formation of tight chemical bonds between the bioactive materials and the neighbouring tissues.[22] The bonelike HCA layer can be reproduced in SBF and previous studies have shown that

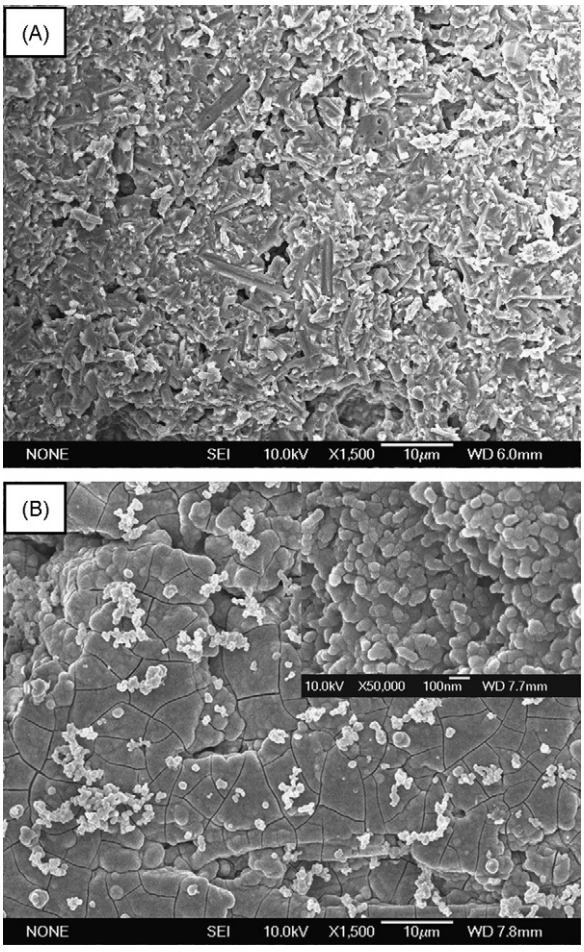

Fig. 3. FESEM micrographs of the surface of the 45BG-reinforced MCSCs soaked in SBF for 0 (A) and 1 (B) day.

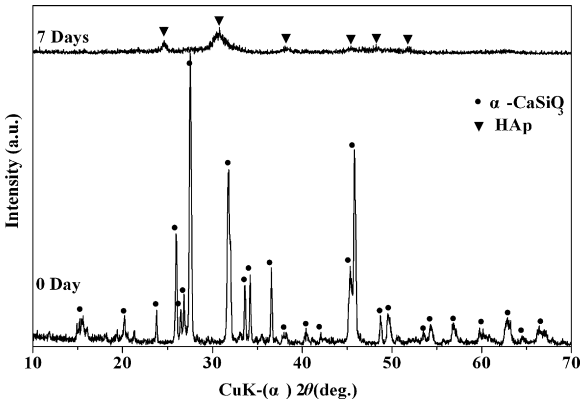

Fig. 4. XRD patterns of the 45BG-reinforced MCSCs soaked in SBF for 0 and 7 days.

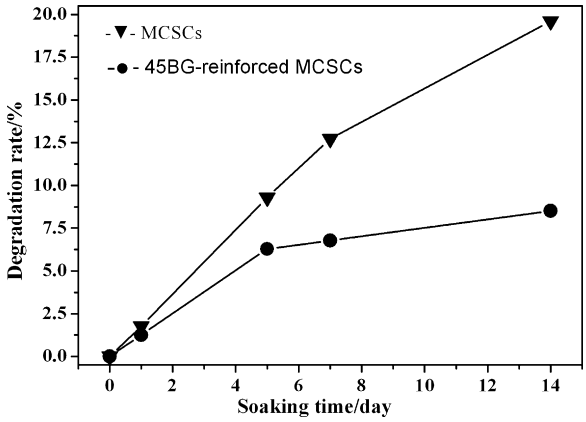

Fig. 6. The degradation rate of the MCSCs and 45BG-reinforced MCSCs in SBF.

Bioglass, AW bioceramics, $CaSiO_3$, Ca_2SiO_4 etc. can induce the HCA deposition when soaked in SBF and can be used as bioactive materials in clinical applications.[8–11,20,22,28] Therefore, the 45BG-reinforced MCSCs could be potential candidates for bioactive scaffolds in biomedical applications.

Degradability is another important requirement for the third-generation biomaterials.[1] Corresponding to the Si concentration in SBF after soaking the samples, the quantitative degradability of the pure MCSCs and 5 wt.% 45BG-reinforced MCSCs were calculated and the results are shown in Fig. 6. It is clear to see that the degradation increases with the increase of the soaking time. The degradation rate of the BG-reinforced MCSCs reached only 1.25% on day 1. With an increase in the soaking time, the degradation increased rapidly in the first few days, and reached 6.29% on day 5, then it increased gradually and reached 6.81% on day 14. In contrast, the degradation of the pure MCSC samples was much faster than that of 45S5 bioglass reinforced samples. On day 1, it reached 1.77%. With the increase of the soaking time, the degradation increased sharply, and reached 19.60% on day 14. The results show that the extent of degradation is approximately 3 times higher for the pure MCSC samples than for the 45BG-reinforced MCSCs. The degradation rate of the biodegradable bioceramics is determined by many factors, such as sintering parameters, micro-pore structure and porosity etc.

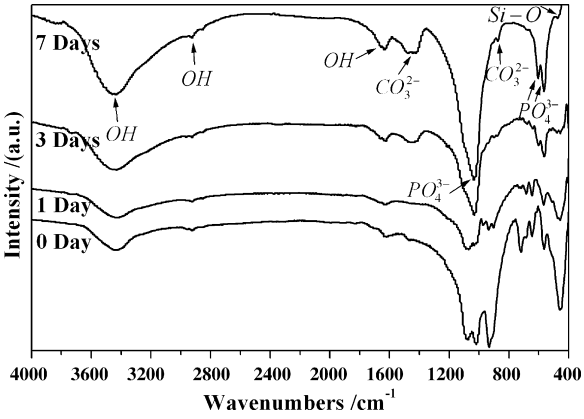

Fig. 5. FTIR spectra of the 45BG-reinforced MCSCs soaked in SBF for various periods.

The micro-pores and porosity play dominant roles in the degradation of ceramics. With the increase of the micro-pore amount and porosity, the degradation rate increases apparently.[29–31] Previous studies suggested that the degradation mechanism of the biodegradable bioceramics is mainly the solution dissolution, and the dissolution always occurs easily on the boundary of the open micro-pores.[29,30] The 45S5 bioglass additives increased the sintering ability of the $CaSiO_3$, which resulted in almost the fully densified solid walls. In contrast, the solid walls of the sintered pure macroporous $CaSiO_3$ scaffolds possessed large amount of micro-pores. Therefore, the degradation rate of the pure MCSCs was much faster than that of 45BG-reinforced MCSCs. Furthermore, the degradability of the 45BG-reinforced MCSCs was just about one-third of those pure MCSCs, which indicated that the degradability of $CaSiO_3$ bioceramic scaffolds also could be regulated by bioglass additives. The previous studies showed that a major drawback of the $CaSiO_3$ bioceramics is their high dissolution and degradation rate leading to a high pH value in the surrounding environment,[9,32] which can disadvantage cell growth thereby affecting their osseointegration ability.[33] Therefore, using 45S5 bioglass as reinforcement additives might be one of the effective approaches for decreasing the dissolution and degradation rate of $CaSiO_3$ bioceramics, which might be an effective approach to improve the osseointegration ability.

4. Conclusions

In this study, 5 wt.% 45S5 bioglass reinforced macroporous $CaSiO_3$ ceramics (45BG-reinforced MCSCs) with evenly distributed and interconnected pores were fabricated. The 45S5 bioglass additive was found to effectively enhance the strength of the macroporous $CaSiO_3$ ceramics by the liquid-phase sintering mechanism. The optimum amount of bioglass was 5 wt.% and the compressive strength of the reinforced samples was approximately 2 times higher than that of pure macroporous calcium silicate ceramics (MCSCs). The open porosities and compressive strength of the reinforced samples could be manipulated by varying the weight fraction of the porogens. An increase of 10 wt.% of PEG could result in a 10% increase of open porosity.

The compressive strength of the 45BG-reinforced MCSCs could be controlled between 8.74 and 112.47 MPa through regulation of the weight fraction of the porogens. The compressive strength of the reinforced samples with about 50% porosity reached 112.47 MPa, which was similar to that of the cortical bones. When soaked in SBF, the bonelike hydroxycarbonate apatite (HCA) was deposited on the surface of the samples. Furthermore, the degradation rate of 45BG-reinforced MCSCs was just about one-third of those pure MCSCs, indicating that the degradability of $CaSiO_3$ bioceramic scaffolds also could be regulated by the bioglass additives. Our results indicated that degradable 45BG-reinforced MCSC scaffolds possess excellent mechanical strength and bioactivity, and could be potential candidates for hard tissue prosthetics or bone tissue engineering applications.

Acknowledgements

This work was supported by grants from Science and Technology Commission of Shanghai Municipality (Grant Nos.: 07ZD05012 and 07ZR14127), the National Basic Research Program (<973> Program) of PR China (Grant No.: 2005CB522704) and Knowledge Innovation Program (Grant No.: SCX200704) of the Chinese Academy of Sciences.

References

[1]. Hench, L. L. and Polak, J. M., Third-generation biomedical materials. *Science*, 2002, **295**, 1014–1017.
[2]. Flatley, T. J., Lynch, K. L. and Benson, M., Tissue response to implants of calcium phosphate ceramic in the rabbit spine. *Clin. Orthop.*, 1983, **179**, 246–252.
[3]. Chang, B. S., Lee, C. K., Hong, K. S., Youn, H. J., Ryu, H. S., Chung, S. S. and Park, K. W., Osteoconduction at porous hydroxyapatite with various pore configurations. *Biomaterials*, 2000, **21**, 1291–1298.
[4]. Ducheyne, P., Bioceramics: material characteristics versus in vivo behavior. *J. Biomed. Mater. Res.*, 1987, **21**, 219–236.
[5]. De Aza, P. N., Luklinska, Z. B., Martinez, A., Anseau, M. R., Guitian, F. and De Aza, S., Morphological and structural study of pseudowollastonite implants in bone. *J. Microsc.*, 2000, **197**, 60–67.
[6]. Xue, W. H., Liu, X. Y., Zheng, X. B. and Ding, C. X., In vivo evaluation of plasma-sprayed wollastonite coating. *Biomaterials*, 2005, **26**, 3455–3460.
[7]. Xu, S. F., Lin, K. L., Hu, Y. Y., Wang, Z., Chang, J., Wang, L., Lu, J. X. and Ning, C. Q., Reconstruction of calvarial defect of rabbits using porous calcium silicate bioactive ceramics. *Biomaterials*, 2008, **29**, 2588–2596.
[8]. Liu, X. Y., Ding, C. X. and Chu, P. K., Mechanism of apatite formation on wollastonite coatings in simulated body fluids. *Biomaterials*, 2004, **25**, 1755–1761.
[9]. Siriphannon, P., Hayashi, S., Yasumori, A. and Okada, K., Preparation and sintering of $CaSiO_3$ from coprecipitated powder using NaOH as precipitant and its apatite formation in simulated body fluid solution. *J. Mater. Res.*, 1999, **14**, 529–536.
[10]. Lin, K. L., Chang, J. and Wang, Z., Fabrication and the characterization of the bioactivity and degradability of macroporous calcium silicate bioceramics in vitro. *J. Inorg. Mater.*, 2005, **20**, 692–698.
[11]. Ohtsuki, C., Miyazaki, T., Kamitakahara, M. and Tanihara, M., Design of novel bioactive materials through organic modification of calcium silicate. *J. Eur. Ceram. Soc.*, 2007, **27**, 1527–2533.
[12]. Sarmento, C., Luklinska, Z. B., Brown, L., Anseau, M., De Aza, P. N. and De Aza, S., In vitro behavior of osteoblastic cells cultured in the presence of pseudowollastonite ceramic. *J. Biomed. Mater. Res. A*, 2004, **69**, 351–358.
[13]. Lin, K. L., Chang, J., Zeng, Y. and Qian, W. J., Preparation of macroporous calcium silicate ceramics. *Mater. Lett.*, 2004, **58**, 2109–2113.
[14]. Hench, L. L. and Wilson, J., *An Introduction to Bioceramics*. World Scientic, London, UK, 1993.
[15]. Oktara, F. N. and Goller, G., Processing and characterization of bioglass reinforced hydroxyapatite composites. *Ceram. Int.*, 2003, **29**, 721–724.
[16]. Suchanek, W., Yashima, M., Kakihana, M. and Yoshimura, M., Hydroxyapatite ceramics with selected sintering additives. *Biomaterials*, 1997, **18**, 923–933.
[17]. Kingery, W. D., Densification during sintering in the presence of a liquid phase. I. Theory. *J. Appl. Phys.*, 1959, **30**, 301–307.
[18]. Montazerian, M., Alizadeh, P. and Eftekhari Yekta, B., Pressureless sintering and mechanical properties of mica glass–ceramic/Y-PSZ composite. *J. Eur. Ceram. Soc.*, 2008, **28**, 2687–2692.
[19]. Goller, G., Demirkiran, H., Oktar, F. N. and Demirkesen, E., Processing and characterization of bioglass reinforced hydroxyapatite composites. *Ceram. Int.*, 2003, **29**, 721–724.
[20]. Hench, L. L. and Bioceramics, *J. Am. Ceram. Soc.*, 1998, **81**, 1705–1728.
[21]. Engin, N. O. and Tas, A. C., Manufacture of macroporous calcium hydroxyapatite bioceramics. *J. Eur. Ceram. Soc.*, 1999, **19**, 2569–2572.
[22]. Kokubo, T. and Takadama, H., How useful is SBF in predicting in vivo bone bioactivity? *Biomaterials*, 2006, **27**, 2907–2915.
[23]. Rice, R. W., Evaluation and extension of physical property—porosity models based on minimum solid area. *J. Mater. Sci.*, 1996, **31**, 102–118.
[24]. Ioku, K., Kurosawa, H., Shibuya, K., Yokozeki, H. and Hayashi, T., *Bioceramics*, *vol. 7*, ed. H. Andersson and Y. Urpo. Butterworth-Heinemann, London, 1994, p. 97.
[25]. Radin, S. R. and Ducheyne, P., Plasma spraying induced changes of calcium phosphate ceramic characteristics and the effect on in vitro stability. *J. Mater. Sci.: Mater. Med.*, 1992, **3**, 33–42.
[26]. Weng, J., Liu, Q., Wolke, J. G. C., Zhang, X. and De Groot, K., Formation and characteristics of the apatite layer on plasma-sprayed hydroxyapatite coatings in simulated body fluid. *Biomaterials*, 1997, **18**, 1027–1035.
[27]. Fowler, B. O., Infrared studies of apatite. I. Vibrational assignments for calcium, strontium and barium hydroxyapatites utilizing isotopic substitution. *Inorg. Chem.*, 1974, **13**, 194–214.
[28]. Gou, Z. R., Chang, J. and Zhai, W. Y., Preparation and characterization of novel bioactive dicalcium silicate ceramics. *J. Eur. Ceram. Soc.*, 2005, **25**, 1507–1514.
[29]. Koerten, H. K. and Van-Der Meulen, J., Degradation of calcium phosphate ceramics. *J. Biomed. Mater. Res.*, 1999, **44**, 78–86.
[30]. Klein, C. P. A. T., Driessen, A. A. and De Groot, K., Biodegradation behavior of various calcium phosphate materials in bone tissue. *J. Biomed. Mater. Res.*, 1983, **17**, 769–784.
[31]. Cameron, H. U., MacNab, I. and Pillar, R. M., Evaluation of a biodegradable ceramic. *J. Biomed. Mater. Res.*, 1977, **11**, 179–185.
[32]. Iimori, Y., Kameshima, Y., Okada, K. and Hayashi, S., Comparative study of apatite formation on $CaSiO_3$ ceramics in simulated body fluids with different carbonate concentrations. *J. Mater. Sci.: Mater. Med.*, 2005, **16**, 73–79.
[33]. El-Ghannam, A., Ducheyne, P. and Shapiro, I. M., Formation of surface reaction products on bioactive glass and their effects on the expression of the osteoblastic phenotype and the deposition of mineralized extracellular matrix. *Biomaterials*, 1997, **18**, 295–303.